International Journal of Statistics and Applied Mathematics 2022; 7(3): 155-166

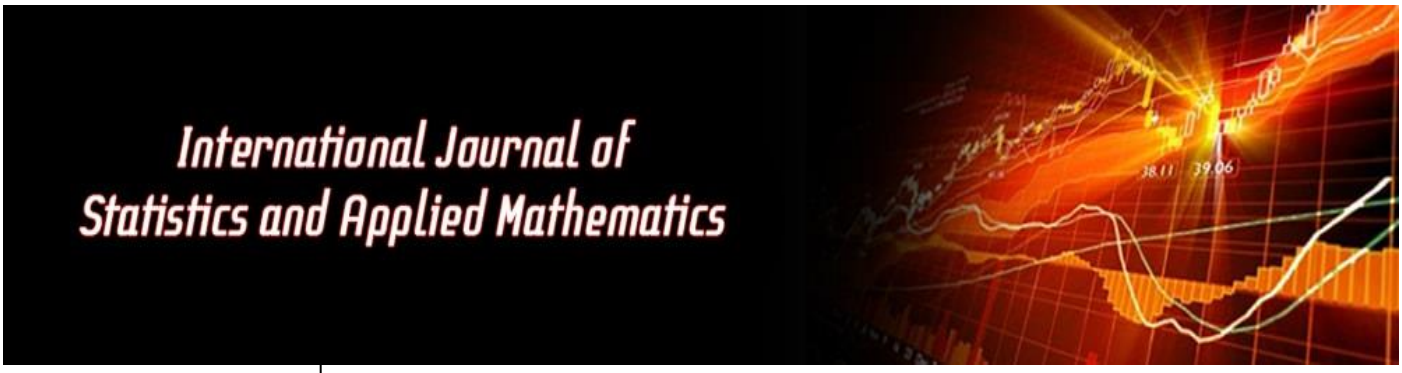

ISSN: 2456-1452
Maths 2022; 7(3): 155-166

www.mathsjournal.com
Received: 12-03-2022
Accepted: 16-04-2022

KW Bunonyo
Mathematical Modeling and Data Analytic Research Group (MMDARG), Department of Mathematics and Statistics, Federal University, Otuoke, Nigeria

UC Amadi
Department of Mathematics and Statistics, Federal University, Otuoke, Nigeria

Corresponding Author:
KW Bunonyo
Mathematical Modeling and Data Analytic Research Group (MMDARG), Department of Mathematics and Statistics, Federal University, Otuoke, Nigeria

Oscillatory electro-hydrodynamic (EHD) fluid flow through a microchannel in the presence of radiative heat and a magnetic field

KW Bunonyo and UC Amadi

DOI: https://doi.org/10.22271/maths.2022.v7.i3b.836

Abstract
In this article, we investigated the oscillatory flow of an electo-hydrodynamic fluid flow through a channel with a radiative heat and magnetic field. The momentum equation, energy equation, and lipid concentration equation were used to represent the problem under consideration. The dimensionless equations were reduced to ordinary differential equations using the oscillatory perturbation parameters after the partial differential equations were scaled to be dimensionless. The ordinary differential equations are directly solved.
We obtained some governing parameters during the analysis of the solution, such as thermal Grashof number, nanoparticles Grashof number, Reynolds number, wave number, radiation absorption parameter, thermophoresis parameter, electroosmotic parameter, and Schmidt number, respectively. The study was conducted to investigate the effects of the aforementioned parameters on the various flow profiles, and the results showed that the Grashof number, electroosmotic, and thermophoresis caused the fluid velocity to increase after varying them within a specific range, whereas the Brownian parameter, Reynolds number, and wave number caused the velocity to decrease. The thermophoresis and electroosmotic parameter values, on the other hand, raise the temperature of the fluid. Finally, we were able to develop a coupled system of mathematical models that represent electro-hydrodynamic fluid flow through a channel, solve it, and obtain exact solutions for the velocity profile, temperature profile, and lipid concentration profile.

Keywords: Oscillatory, electro-hydrodynamic, microchannel, magnetic field, radiative heat, electroosmotic fluid, momentum equation, lipid concentration equation

1. Introduction
According to Resuss, an electrokinetic phenomenon, also known as electroosmosis or electro-osmotic flow (EOF), is defined as the flow of fluid in any conduit (e.g., microchannel, capillary tube) under the influence of an external electric field (1809) [1]. Micro-flow injection analysis, micro-liquid chromatography, and micro-energy systems all benefit from EOF. Other authors' research is included below. Patankar *et al.* 1998 [2] studied the electro-osmotic flow through a microchannel. Yang *et al.* 2021 [3] investigated EOF in microfluidics. Tang *et al.* 2009 [4] investigated the EOF in the context of a power-law model. Miller *et al.* 2001 [5] predicted EOF using a carbon nanotube membrane later on.
Nanofluids have been found to have improved thermophysical properties (thermal conductivity, thermal diffusivity, and the viscosity of the convective heat transport coefficient) when compared to conventional fluids.
Nano-liquid elements have shown colossal potential applications in many fields. The endoscopic effect of nanofluids in peristalsis was dissected by Akbar *et al.* 2011 [6]. Noreen 2013 [7] explored nanofluids under initiated attractive fields and blended convection. Moreover, Tripathi *et al.* 2014 [8] contemplated the peristaltic movement of nanofluid. Reddy *et al.* (2015) [9] suggested the peristaltic stream of nanofluid through objection dividers. Ebaid *et al.* 2018 [10] inspected the peristaltic movement of nanofluid under convective circumstances. Shao *et al.* 2016 [11] read up a reference answer for twofold dispersion convection. Twofold diffusive convection is a liquid element peculiarity that describes a type of convection driven if at the point when the temperature contrast is held consistent, warm

dispersion delivers a focused inclination. Taking into account the wide uses of twofold diffusive convection, it was concentrated in a nano-fluidic stream model with peristaltic siphoning. Huppert *et al*. 1981 [12] examined the utilization of twofold dispersion convection. Essentially, Bég *et al*. 2011 [13] depicted the peristaltic siphoning of nano-liquids through twofold diffusive convection. Kefayati 2014 [14] made sense of twofold dispersion convection for pseudoplastic liquids. The peristaltic movement of the MHD course through twofold diffusive convection was concentrated by Rout 2014 *et al*. [15]

Unstable electrokinetic transport through peristaltic microchannels was concentrated by Tripathi *et al*. 2016 [16] Tripathi *et al*. 2017 [17] investigated the peristaltic movement of the couple-stress liquid through the microchannel. In Prakash *et al*. 2018 [18] they analyzed the peristaltic movement of Williamson ionic nanofluid in the tightened microchannel. Tripathi *et al*. 2018 [19] likewise concentrated on the blood stream balanced by electroosmosis. Additionally, Tripathi *et al*. 2018 [20] concentrated on the consolidated impact of electroosmosis and peristalsis through the microchannel. Likewise, Tripathi *et al*. 2018 [21] uncovered the peristaltic transport of nanofluids with a light impact by means of a microchannel. The effect of intensity and mass on the joined impact of electroosmosis and peristalsis was concentrated by Waheed *et al.* 2019 [22]. Noreen *et al*. 2019 [23] examined the impact of intensity on EOF through peristaltic siphoning. In another review, Noreen *et al*. 2019 [24] suggested the vehicle of MHD nanofluid through the peristaltic microchannel. Entropy age in peristaltically prompted microchannels is a quickly arising area of interest.

The investigation of entropy within the framework is important because it aids in tracing the sources of available energy. Various sources of irreversibility include intensity course through the limited temperature slope, convective intensity move characteristics, and consistency and dissemination impacts. Entropy can be limited to save energy quality for the ideal plan of any warm framework. As of now, the examination subject of limiting entropy age has acquired unique status among researchers around the world. Restricted examinations have researched the entropy creation in electro-osmotically prompted peristaltic microchannels. Kefayati 2016 [25] made sense of entropy creation for non-Newtonian nanofluids through a permeable depression. Kefayati 2016 [26] has likewise portrayed entropy creation and twofold diffusive convection for power-regulation liquids.

In the previously mentioned referenced works, nobody has had the option to take a gander at them in an oscillatory stream and concoct a consequence of some kind or another. Accordingly, the ongoing examination expects to fill this hole. The discoveries of the current investigation can be utilized for clinical purposes like cell treatment, drug conveyance frameworks, pharmaco-dynamic siphons, and molecule filtration. Likewise, to extend how we might interpret thermosolutal convection, unique consideration was paid to concentrating on entropy age.

2. Mathematical Formulation

The microchannel is restricted by some growth at the upper wall of the channel caused by cholesterol, which causes a periodic wave at a velocity along the axial direction of the channel. The temperature and the nanoparticles at the lower part of the channel are taken as respectively. According to Mohan and Satheesh 2016 [27], the mathematical representation of the geometry at the upper wall is expressed is:

$$h^* = a^* + b^* sin\left(2\pi \frac{\left(x^* - ct^*\right)}{\lambda^*}\right) \tag{1}$$

where h^* represents the transverse vibration of the wall, a^* is the half width of the channel, b^* is the amplitude of the wave caused by the restriction, x^* represent the axial flow direction, λ^* is the wavelength in relation to the restricted area and t^* is the time.

2.1 Mathematical Models

The models governing the physical problem electro-hydrodynamic (EHD) flow of nanofluid through a restricted microchannel with radiative heat following, Bunonyo and Amos 2021 [28] and Noreen *et al.* 2019 [23, 24] are:

$$\rho \frac{\partial w^*}{\partial t^*} = -\frac{\partial P^*}{\partial x^*} - \frac{\mu}{k} w^* + \frac{\partial^2 w^*}{\partial y^{*2}} + \rho_0 \left(1 - F_0\right) g \beta_T \left(T^* - T_0\right) - g\left(\rho_p - \rho_0\right)\left(F^* - F_0\right) + \rho_e E_x \tag{2}$$

$$\rho C_p \frac{\partial T^*}{\partial t^*} = k_T \frac{\partial^2 T^*}{\partial y^{*2}} - Q\left(T^* - T_0\right) \tag{3}$$

$$\frac{\partial F^*}{\partial t^*} = D_b \frac{\partial^2 F^*}{\partial y^{*2}} + \frac{D_t}{T_0} \frac{\partial^2 F^*}{\partial y^{*2}} \tag{4}$$

The Poisson-Boltzmann equation according to Tripathi *et al.* 2017 [17] is

$$\frac{\partial^2 \phi^*}{\partial y^{*2}} = -\frac{\rho_e}{\varepsilon} \tag{5}$$

The transformational and the dimensionless parameters are:

$$\left.\begin{aligned} &x^* = x\lambda^*, y^* = \alpha\lambda y, a^* = \alpha\lambda, t^* = \frac{\lambda t}{c}, P^* = \frac{P\mu c}{\alpha^2\lambda}, \varepsilon = \frac{b^*}{a^* e^{\alpha t}}, Re = \frac{c\lambda}{\upsilon}, \\ &w^* = wc, h^* = ha^*\theta = \frac{T^* - T_0}{T_0}, \gamma = \frac{F^* - F_0}{F_0}, \phi^* = \frac{\phi T_{av} k_B}{ez_v}, u_{hs} = \frac{T_{av} k_B \varepsilon E_x}{ez_v c\mu}, \\ &Q^* = \frac{Q_0}{\alpha^2 \lambda^{*2}}, Pr = \frac{\mu c_p}{k_T}, Nb = D_b \frac{\left(\rho c_p\right)_p F_0}{k_T}, Nt = D_t \frac{\left(\rho c_p\right)_p}{k_T}, S_b = \frac{ca^*}{D_b}, \\ &Grf = \frac{ga^*\left(\rho_p - \rho_0\right)F_0}{c\mu}, Grt = \frac{\rho_0 g a^{*2} T_0 \left(1 - F_0\right)}{c\mu} \end{aligned}\right\} \quad (6)$$

Using equation (6) in simplifying equations (1)-(5), we have the following:

$$h(x) = 1 + \varepsilon e^{\alpha t} \sin 2\pi x \quad (7)$$

$$Re\alpha^2 \frac{\partial w}{\partial t} = -\frac{\partial P}{\partial x} + \frac{\partial^2 w}{\partial y^2} + Gr_t\theta - Gr_f\gamma - u_{hs}\frac{d^2\phi}{dy^2} \quad (8)$$

$$Pr\alpha^2 \frac{\partial \theta}{\partial t} = \frac{\partial^2 \theta}{\partial y^2} - RdPr\theta \quad (9)$$

$$S_b \frac{\partial \gamma}{\partial t} = \frac{\partial^2 \gamma}{\partial y^2} + \frac{N_t}{N_b}\frac{\partial^2 \theta}{\partial y^2} \quad (10)$$

Applying Debye-Huckel linearization approximation according to Prakash and Tripathi (2018) [18] and equation (6), then equation (5) becomes:

$$\frac{d^2\phi}{dy^2} = m_e^2\phi \quad (11)$$

Equations (8)-(11) are subject to the following boundary conditions:

$$\left.\begin{aligned} &\frac{\partial w}{\partial y} = 0, \frac{\partial \phi}{\partial y} = 0, \theta = 0, \gamma = 0 \quad \text{at } y = 0 \\ &w = 0, \phi = 1, \theta = 1, \gamma = 1 \quad \text{at } y = h(x) = 1 + \varepsilon e^{\alpha t}\sin 2\pi x \end{aligned}\right\} \quad (12)$$

3. Method of Solution

Let us assume that the flow is oscillatory in the channel, following Bunonyo and Amos (2020) [29], we present the solution to be the form:

$$\left.\begin{aligned} &w = w_0 e^{i\omega t}, \theta = \theta_0 e^{i\omega t} \\ &\gamma = \gamma_0 e^{i\omega t}, \phi = \phi_0 e^{i\omega t} \end{aligned}\right\} \quad (13)$$

Substituting equation (13) into equations (8)-(12), we have:

$$\frac{d^2\phi_0}{dy^2} = m_e^2\phi_0 \quad (14)$$

$$\frac{\partial^2 w_0}{\partial y^2} - Re\alpha^2 \omega w_0 - P_0 + Gr_t \theta_0 - Gr_f \gamma_0 - u_{hs} m_e^2 \phi_0 = 0 \tag{15}$$

$$\frac{\partial^2 \theta_0}{\partial y^2} - \left(Rd + \alpha^2 \omega\right) Pr \theta_0 = 0 \tag{16}$$

$$\frac{\partial^2 \gamma_0}{\partial y^2} - S_b \omega \gamma_0 + \frac{N_t}{N_b} \frac{\partial^2 \theta_0}{\partial y^2} = 0 \tag{17}$$

Equations (8)-(11) are subject to the following boundary conditions:

$$\left.\begin{aligned} &\frac{\partial w_0}{\partial y} = 0, \frac{\partial \phi_0}{\partial y} = 0, \theta_0 = 0, \gamma_0 = 0 \qquad \text{at } y = 0 \\ &w_0 = 0, \phi_0 = e^{-\omega t}, \theta_0 = e^{-\omega t}, \gamma_0 = e^{-\omega t} \qquad \text{at } y = h(x) = 1 + \varepsilon e^{at} sin 2\pi x \end{aligned}\right\} \tag{18}$$

Solving equation (14), we have

$$\phi_0(y) = A sinh(m_e y) + B cosh(m_e y) \tag{19}$$

Solving equation (19) using the boundary condition in equation (18), we have

$$\phi_0(y) = \frac{cosh(m_e y)}{cosh(m_e h)} e^{-\omega t} \tag{20}$$

Solving equation (16), we have

$$\theta_0(y) = \frac{sinh(\beta_1 y) e^{-\omega t}}{sinh(\beta_1 h)} \tag{21}$$

Where

$$\beta_1^2 = \left(Rd + \alpha^2 \omega\right) Pr$$

Differentiate equation (21) twice and substitute the result into equation (17), which is

$$\frac{\partial^2 \gamma_0}{\partial y^2} - S_b \omega \gamma_0 = -\left(\frac{\beta_1^2 N_t e^{-\omega t}}{N_b sinh(\beta_1 h)}\right) sinh(\beta_1 y) \tag{22}$$

The homogenous and particular solutions of equation (22) are

$$\gamma_{0h}(y) = A_2 sinh(\beta_2 y) + B_2 cosh(\beta_2 y) \tag{23}$$

$$\gamma_{0p}(y) = \left(\frac{1}{\left(\beta_2^2 - \beta_1^2\right)}\left(\frac{\beta_1^2 N_t e^{-\omega t}}{N_b sinh(\beta_1 h)}\right)\right) sinh(\beta_1 y) \tag{24}$$

So, the solution to equation (22) is

$$\gamma_0(y) = A_2 sinh(\beta_2 y) + B_2 cosh(\beta_2 y) + \left(\frac{1}{\left(\beta_2^2 - \beta_1^2\right)}\left(\frac{\beta_1^2 N_t e^{-\omega t}}{N_b sinh(\beta_1 h)}\right)\right) sinh(\beta_1 y) \tag{25}$$

Solving equation (25) using the boundary conditions in equation (18), we have

$$\gamma_0(y) = A_2 sinh(\beta_2 y) + \left(\frac{1}{(\beta_2^2 - \beta_1^2)} \left(\frac{\beta_1^2 N_t e^{-\omega t}}{N_b sinh(\beta_1 h)} \right) \right) sinh(\beta_1 y) \tag{26}$$

Where

$$\beta_2^2 = S_b \omega$$

and

$$A_2 = \frac{e^{-\omega t}}{sinh(\beta_2 h)} + \left(\frac{1}{(\beta_1^2 - \beta_2^2)} \left(\frac{\beta_1^2 N_t e^{-\omega t}}{N_b sinh(\beta_2 h)} \right) \right)$$

Substitute equations (20), (21) and (26) into equation (15), we have:

$$\frac{\partial^2 w_0}{\partial y^2} - \beta_3^2 w_0 = \left\{ P_0 - A_3 sinh(\beta_1 y) + (A_2 Grf sinh(\beta_2 y)) + \left(\frac{u_{hs} m_e^2}{cosh(m_e h)} e^{-\omega t} \right) cosh(m_e y) \right\} \tag{27}$$

Where

$$\beta_3^2 = Re\alpha^2 \omega$$

and

$$A_3 = \left(\frac{Grte^{-\omega t}}{sinh(\beta_1 h)} - \left(\frac{Grf}{(\beta_2^2 - \beta_1^2)} \left(\frac{\beta_1^2 N_t e^{-\omega t}}{N_b sinh(\beta_1 h)} \right) \right) \right)$$

The solution to equation (27) is

$$w_0(y) = A_7 e^{\beta_3 y} + A_8 e^{-\beta_3 y} + A_0 + A_4 sinh(\beta_1 y) + A_5 sinh(\beta_2 y) + A_6 cosh(m_e y) \tag{28}$$

Where

$$A_0 = -\frac{P_0}{\beta_3^2}, A_4 = \frac{A_3}{(\beta_3^2 - \beta_1^2)}, A_5 = \frac{A_2 Grf}{(\beta_2^2 - \beta_3^2)}, A_6 = \left(\frac{u_{hs} m_e^2}{(m_e^2 - \beta_3^2) cosh(m_e h)} e^{-\omega t} \right)$$

Solving equation (28) using the boundary condition in equation (18), we have:

$$\begin{aligned} A_7 e^{\beta_3 h} + A_8 e^{-\beta_3 h} &= \phi_3 \\ A_7 \beta_3 - A_8 \beta_3 &= \phi_4 \end{aligned} \tag{29}$$

Where

$$\phi_3 = -A_0 - A_4 sinh(\beta_1 h) - A_5 sinh(\beta_2 h) - A_6 cosh(m_e h) \text{ and } \phi_4 = -A_4 \beta_1 - A_5 \beta_2$$

Solving equation (29), we have

$$A_7 = \frac{\phi_4 e^{-\beta_3 h} + \phi_3 \beta_3}{\beta_3 e^{-\beta_3 h} + \beta_3 e^{\beta_3 h}} \text{ and } A_8 = \frac{\phi_3 \beta_3 - \phi_4 e^{\beta_3 h}}{\beta_3 e^{-\beta_3 h} + \beta_3 e^{\beta_3 h}} \tag{30}$$

The general solution to equation (28) is:

$$w_0(y)=\left(\frac{\phi_4 e^{-\beta_3 h}+\phi_3\beta_3}{\beta_3 e^{-\beta_3 h}+\beta_3 e^{\beta_3 h}}\right)e^{\beta_3 y}+\left(\frac{\phi_3\beta_3-\phi_4 e^{\beta_3 h}}{\beta_3 e^{-\beta_3 h}+\beta_3 e^{\beta_3 h}}\right)e^{-\beta_3 y}+A_0+A_4 sinh(\beta_1 y)+A_5 sinh(\beta_2 y)+A_6 cosh(m_e y) \quad (31)$$

The velocity prolife is obtained after substituting equation (29) into equation (13), we have

$$w(y,t)=\left(\left(\frac{\phi_4 e^{-\beta_3 h}+\phi_3\beta_3}{\beta_3 e^{-\beta_3 h}+\beta_3 e^{\beta_3 h}}\right)e^{\beta_3 y}+\left(\frac{\phi_3\beta_3-\phi_4 e^{\beta_3 h}}{\beta_3 e^{-\beta_3 h}+\beta_3 e^{\beta_3 h}}\right)e^{-\beta_3 y}+A_0+A_4 sinh(\beta_1 y)+A_5 sinh(\beta_2 y)+A_6 cosh(m_e y)\right)e^{\omega t} \quad (32)$$

The nanoparticles concentration is obtained after substituting equation (13) into equation (26), we have

$$\gamma(y,t)=\left(A_2 sinh(\beta_2 y)+\left(\frac{1}{(\beta_2^2-\beta_1^2)}\left(\frac{\beta_1^2 N_t e^{-\omega t}}{N_b sinh(\beta_1 h)}\right)\right)sinh(\beta_1 y)\right)e^{\omega t} \quad (31)$$

The temperature profile is obtained after substituting equation (21) into equation (13), we have

$$\theta(y)=\left(\frac{sinh(\beta_1 y)e^{-\omega t}}{sinh(\beta_1 h)}\right)e^{\omega t} \quad (32)$$

The electric potential distribution is obtained after substituting equation (20) into equation (13), we have

$$\phi=\left(\frac{cosh(m_e y)}{cosh(m_e h)}e^{-\omega t}\right)e^{\omega t} \quad (33)$$

4. Results

This article showed analytical solution of the formulated problem and numerical simulation done using Wolfram Mathematica, version 12. The parameters values using in the simulations are:

$$Grt=15, Nb=1, Grf=15, Sb=2, Rd=3, Re=5, \alpha=2, Pr=3, Uhs=2, me=2, a=0.5, \varepsilon=0.4, \omega=1,$$

$$t=5, P_0=0.05, x=0.5,$$

and the parameters values are varied to study the effects on various flow profiles. Below are the results:

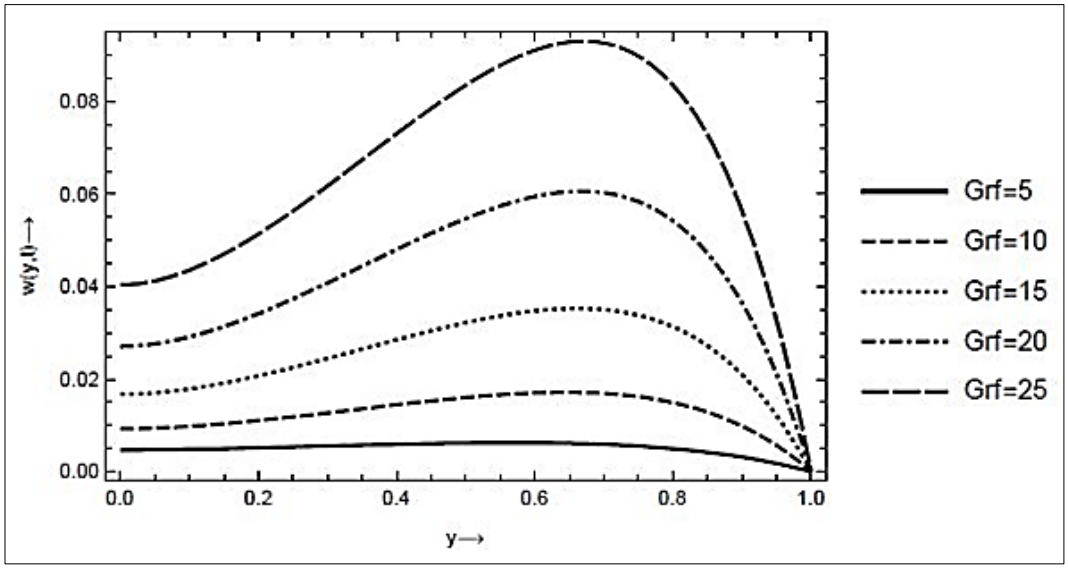

Fig 1: The Effect of thermal Grashof number on velocity profile, with $Grt=15, Nb=1, Nt=1, Sb=2, Rd=3, Re=5, \alpha=2, Pr=3, Uhs=2, me=2, a=0.5, \varepsilon=0.4, \omega=1, t=5, P_0=0.05, x=0.5$

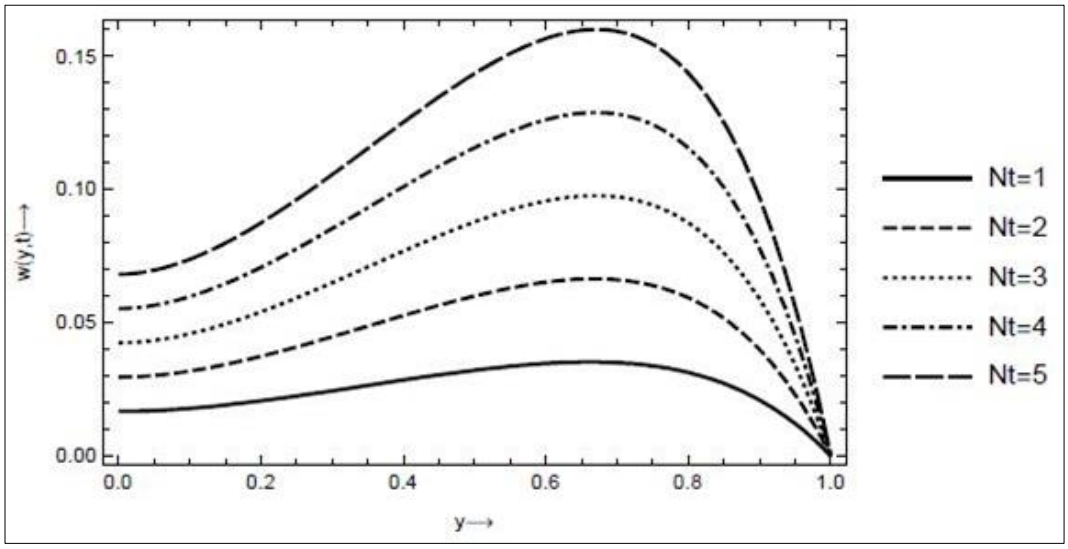

Fig 2: The effect of thermophoresis parameter on velocity profile, with $Grt = 15, Nb = 1, Grf = 15, Sb = 2, Rd = 3, Re = 5, \alpha = 2, Pr = 3, Uhs = 2, me = 2, a = 0.5, \varepsilon = 0.4, \omega = 1, t = 5, P_0 = 0.05, x = 0.5$

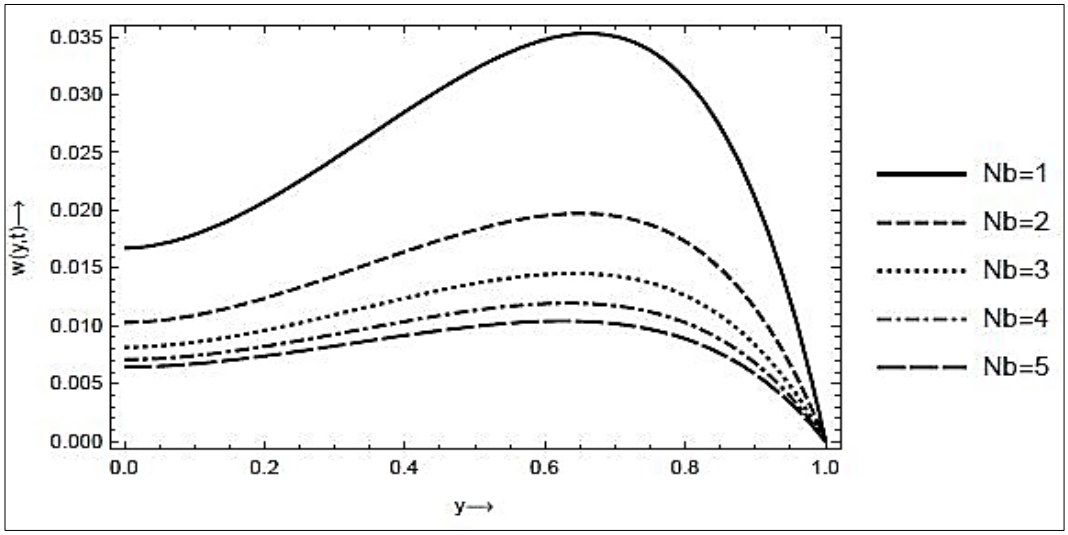

Fig 3: The effect of Brownian motion parameter on velocity profile, with $Grt = 15, Grf = 15, Nt = 1, Sb = 2, Rd = 3, Re = 5, \alpha = 2, Pr = 3, Uhs = 2, me = 2, a = 0.5, \varepsilon = 0.4, \omega = 1, t = 5, P_0 = 0.05, x = 0.5$

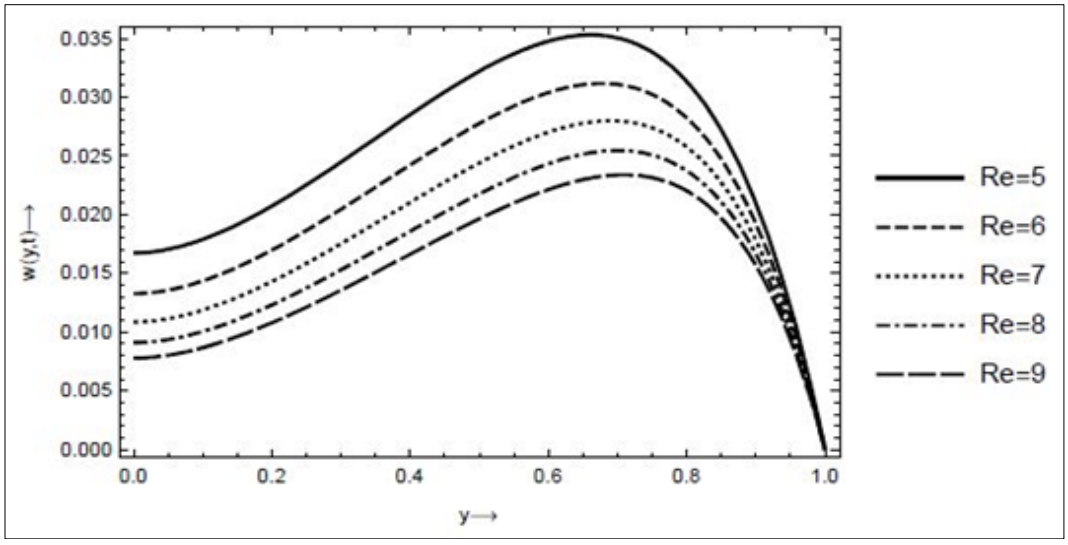

Fig 4: The effect of Reynolds number on velocity profile, with $Grt = 15, Nb = 1, Nt = 1, Sb = 2, Rd = 3, Grf = 15, \alpha = 2, Pr = 3, Uhs = 2, me = 2, a = 0.5, \varepsilon = 0.4, \omega = 1, t = 5, P_0 = 0.05, x = 0.5$

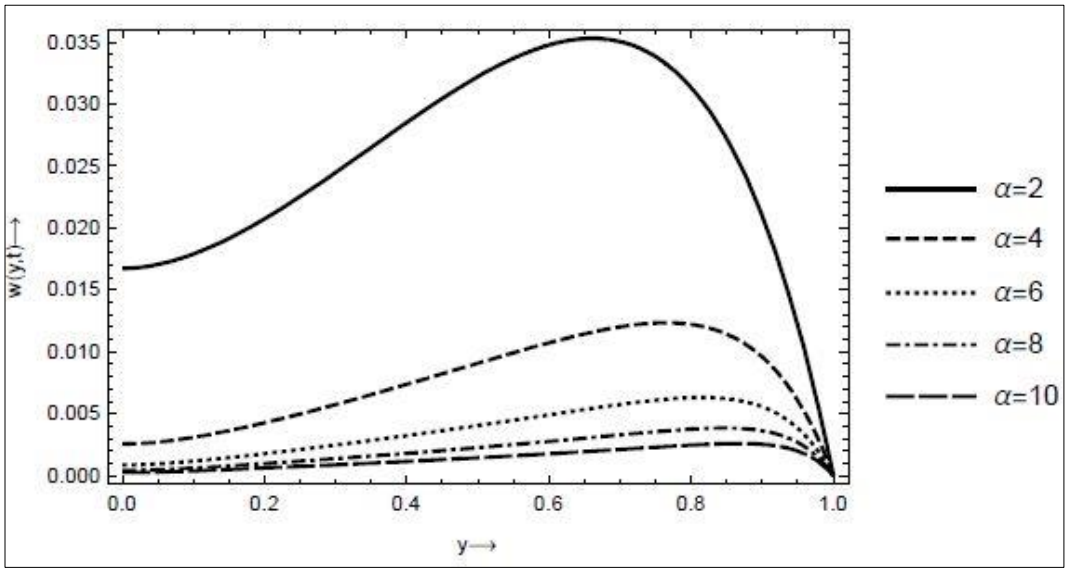

Fig 5: The effect of wave number on velocity profile, with $Grt = 15, Nb = 1, Nt = 1, Sb = 2, Rd = 3, Re = 5, Grf = 15, Pr = 3, Uhs = 2, me = 2, a = 0.5, \varepsilon = 0.4, \omega = 1, t = 5, P_0 = 0.05, x = 0.5$

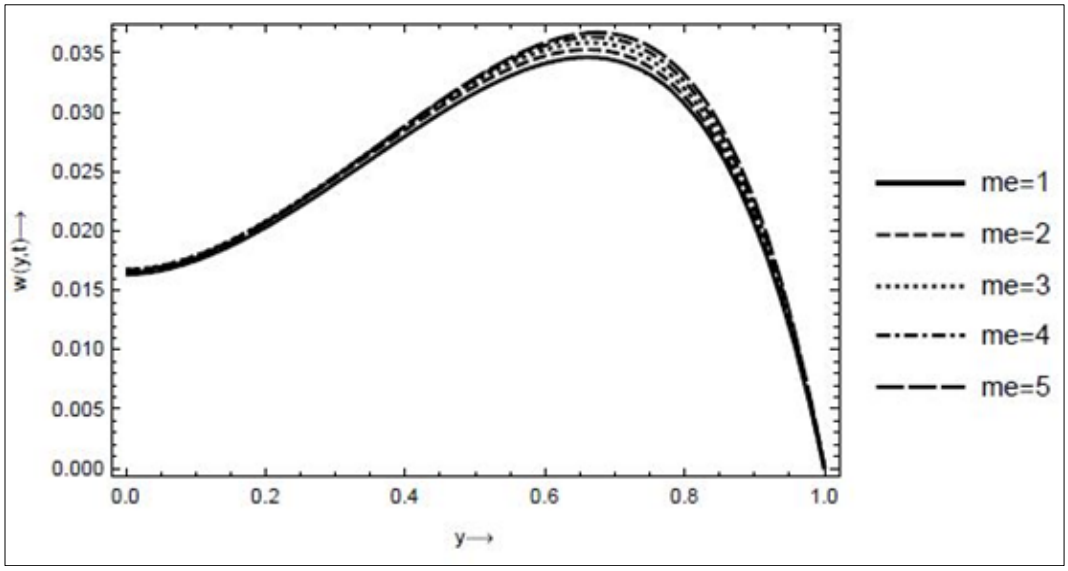

Fig 6: The effect of electroosmotic parameter on velocity profile, with $Grt = 15, Nb = 1, Nt = 1, Sb = 2, Rd = 3, Re = 5, \alpha = 2, Pr = 3, Uhs = 2, Grf = 15, a = 0.5, \varepsilon = 0.4, \omega = 1, t = 5, P_0 = 0.05, x = 0.5$

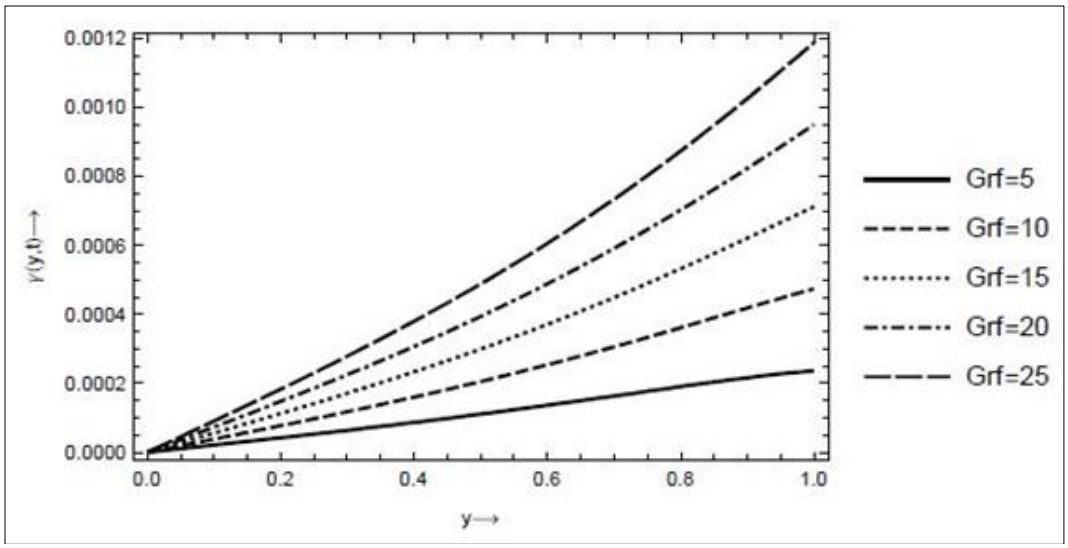

Fig 7: The effect of nanoparticles Grashof number on nanoparticles fraction profile, with $Nb = 1, Nt = 1, Sb = 2, Rd = 2, \alpha = 3, Pr = 2.1, a = 2, \varepsilon = 3, \omega = 2, t = 5, x = 0.5$

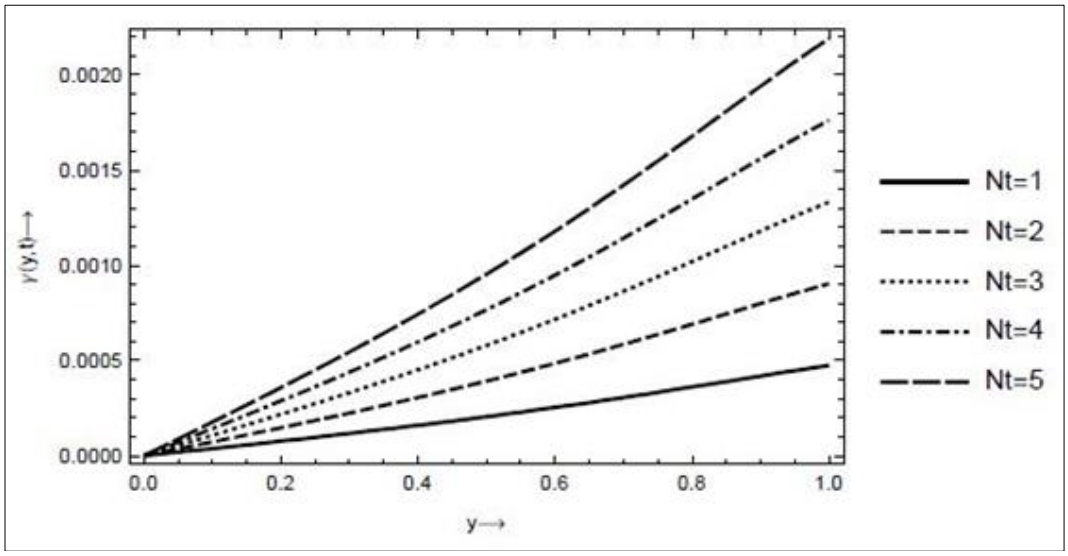

Fig 8: The effect of thermophoresis on nanoparticles fraction profile, with
$Nb=1, Nt=1, Sb=2, Rd=2, \alpha=3, Pr=2.1, a=2, \varepsilon=3, \omega=2, t=5, x=0.5$

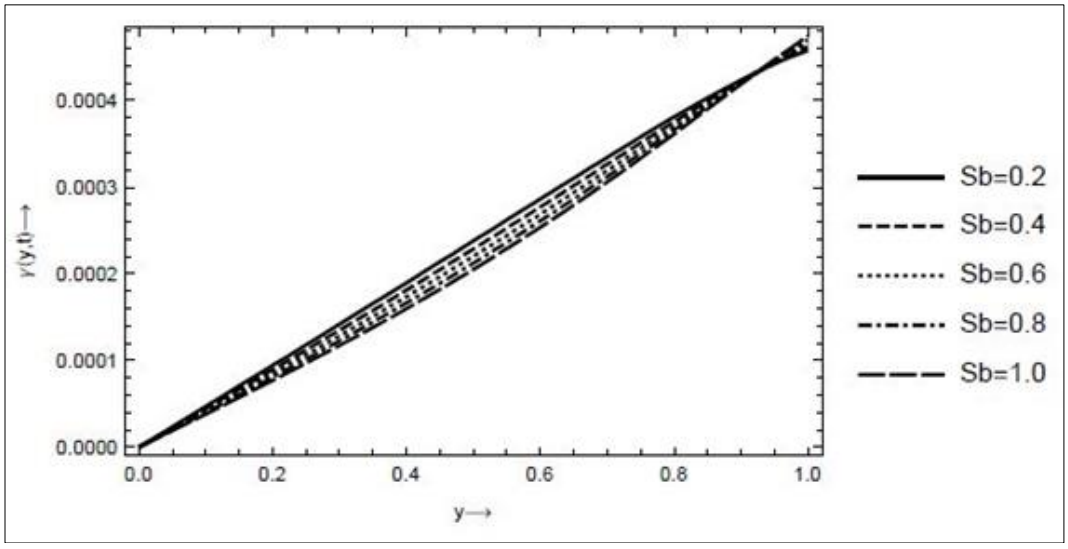

Fig 9: The effect of Schmidt number on nanoparticles fraction profile, with
$Nb=1, Nt=1, Sb=2, Rd=2, \alpha=3, Pr=2.1, a=2, \varepsilon=3, \omega=2, t=5, x=0.5$

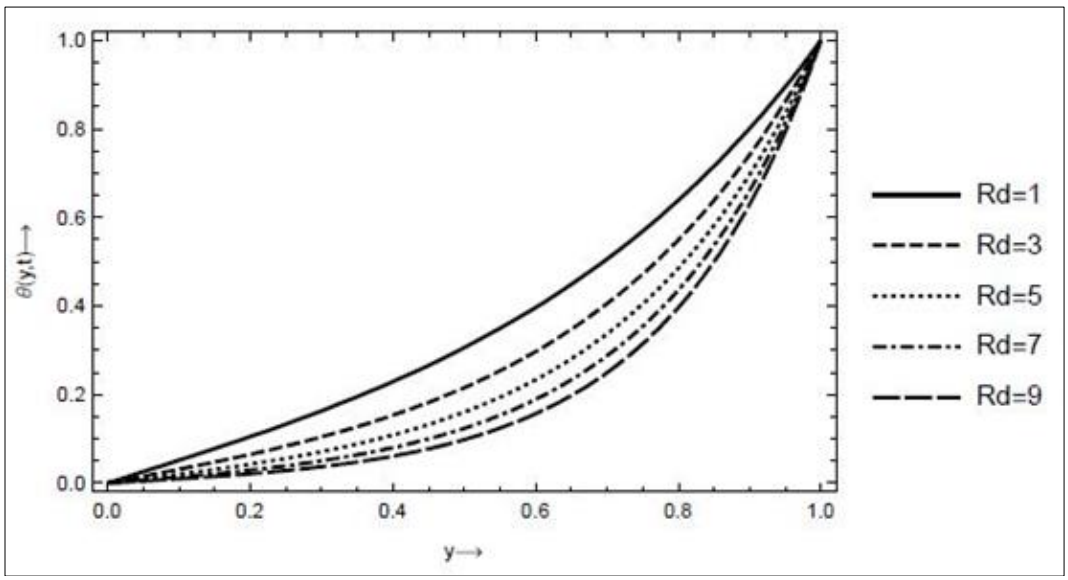

Fig 10: The effect of radiation absorption on temperature profile, with $\alpha=2, Pr=2.1, a=3, \varepsilon=0.001, \omega=0.3, t=5, x=0.5$

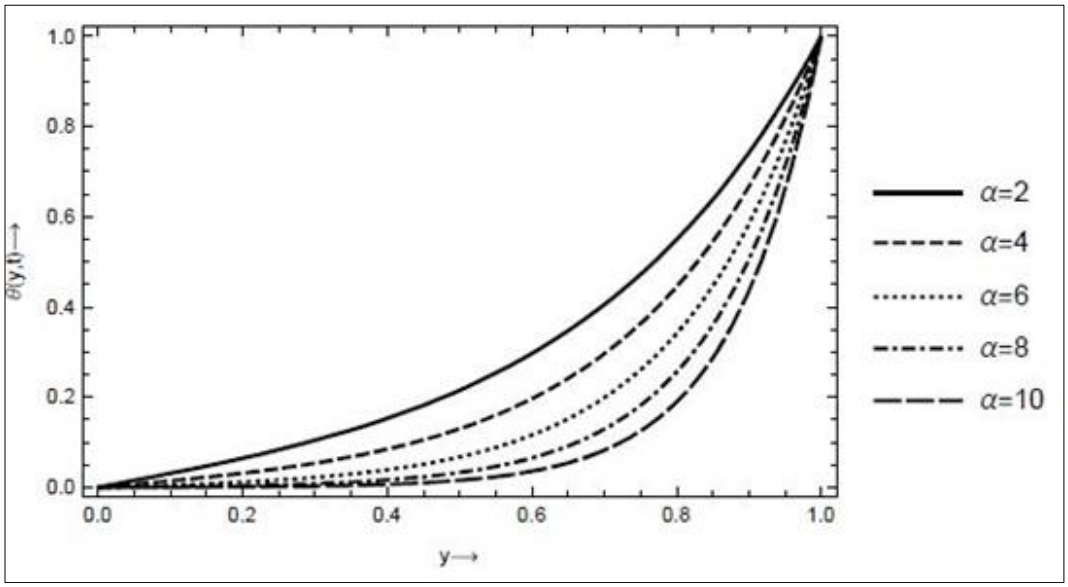

Fig 11: The effect of wave number on temperature profile, with $Rd = 3, Pr = 2.1, a = 3, \varepsilon = 0.001, \omega = 0.3, t = 5, x = 0.5$

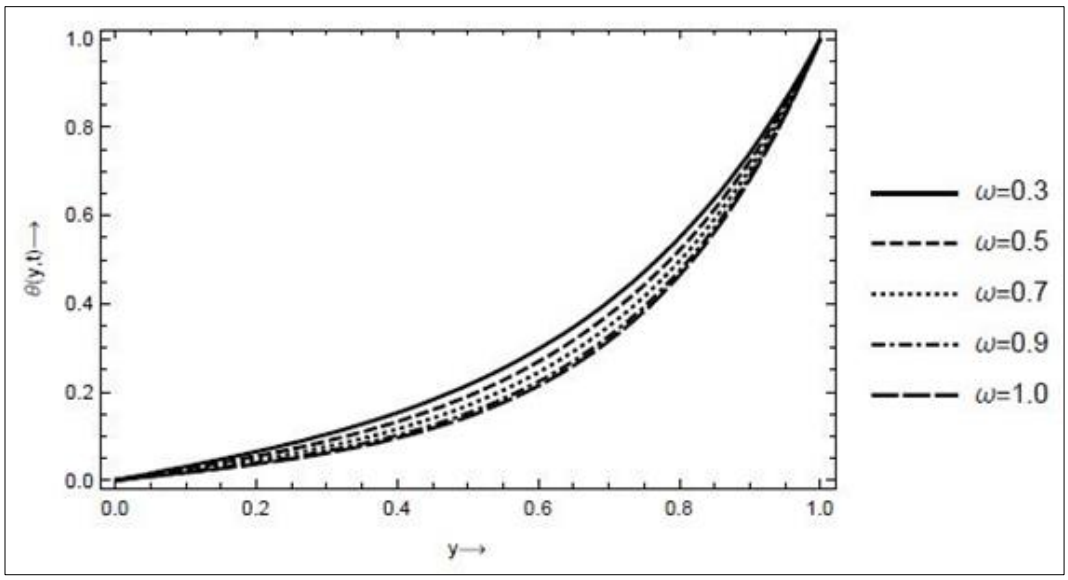

Fig 12: The effect of oscillatory parameter on temperature profile, with $\alpha = 2, Pr = 2.1, a = 3, \varepsilon = 0.001, Rd = 3, t = 5, x = 0.5$

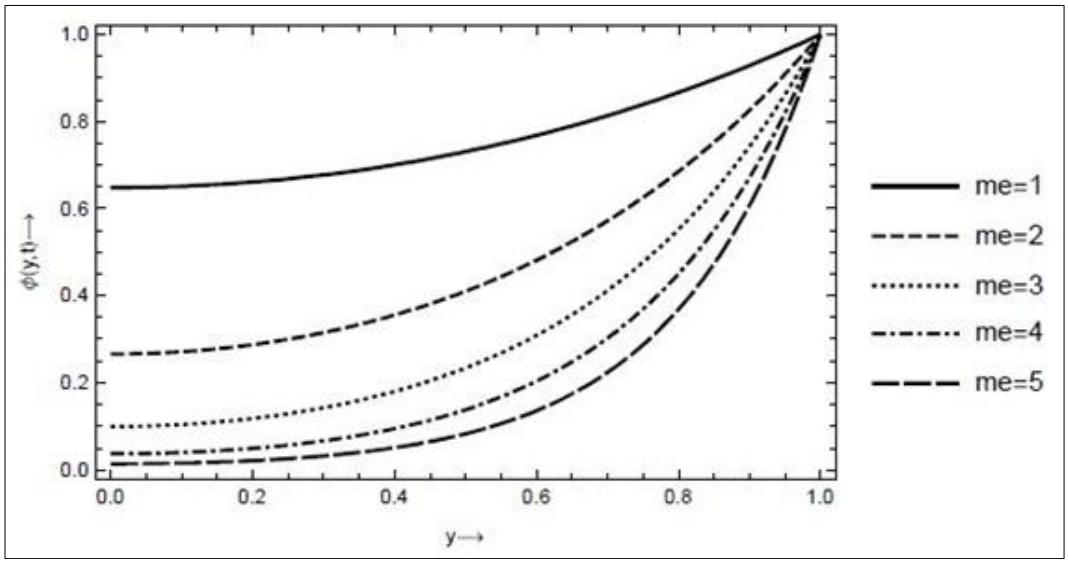

Fig 13: The effect of an electroosmotic values on concentration profile, with $\alpha = 3, \varepsilon = 2.1, t = 5, x = 0.5$

5. Discussion of Results

Fig 1. shows the impact of the warm Grashof number on the liquid speed. It can be seen that the speed increases in order to increase the benefits of the warm Grashof number while other relevant qualities remain constant. The impact of thermophoresis on speed is outlined in Fig 2. The figure shows that the liquid speed increments for expanding upsides of the boundary. Fig 3 shows that the liquid speed diminishes with an expansion in the Brownian boundary. The impact of Reynolds number on the speed profile was explored to significantly affect the liquid speed, as found in Fig 4. The wave number was additionally explored, and it is found in Fig 5 that the speed of the liquid declines for an expansion in wave number. Fig 6 shows that the speed profile of the liquid increments for an expansion in electroosmotic esteem. The impact of the nanoparticles' Grashof number on the nanoparticles' part profile was displayed in Fig 7, and the figure showed that the expansion in Grashof number likewise expands the portion profile. Fig. 8 represents the part profile increments for an expansion in thermophoresis with other contributing boundary values. Regardless, we observed a decrease in part profile for an increase in nano-Schmidt number, as shown in Fig 9. Fig 10. shows the impact of radiation retention on liquid temperature, and it shows that the liquid temperature diminishes with an expansion in radiation assimilation. The wave number impact was likewise examined, and the outcome is found in Fig 11. The result shows that the liquid temperature diminishes for an expansion in wave number. Fig 12. demonstrates the impact of the oscillatory recurrence on the liquid temperature. It is seen that the liquid temperature diminishes with an expansion in the oscillatory recurrence boundary. The electroosmotic esteem significantly affects the lipid fixation in the liquid, and the focus diminishes as the electroosmotic boundary increments, as displayed in Fig 13.

6. Conclusion

The study was carried out to investigate the oscillatory flow of an electro-hydrodynamic (EHD) fluid flow through a microchannel with radiative heat and magnetic field by representing the problem mathematically. The analytical solutions were analyzed and simulation was done using Wolfram Mathematica, focusing on varying the pertinent parameters, and the results were revealed as follows:

1. The thermal Grashof number, electroosmotic and thermophoresis values increase the fluid velocity.
2. The fluid velocity decreases as the Brownian parameter increases.
3. Reynolds number and wave number increases cause a decrease in fluid velocity.
4. An increase in nanoparticles, the Grashof number, increases the fluid temperature.
5. Thermophoresis increased and caused an increase in fluid temperature.
6. The Schmidt number increase decreases the fluid temperature.
7. The electroosmotic value increase caused the lipid concentration in the fluid to increase.

7. References

1. Reuss FF. Charge-induced flow. Proceedings of the Imperial Society of Naturalists of Moscow. 1809;1809(3):327-344.
2. Patankar NA, Hu HH. Numerical simulation of electroosmotic flow. Analytical Chemistry. 1998;70(9):1870-1881.
3. Yang RJ, Fu LM, Lin YC. Electroosmotic flow in microchannels. Journal of colloid and interface science. 2001;239(1):98-105.
4. Tang GH, Li XF, He YL, Tao WQ. Electroosmotic flow of non-Newtonian fluid in microchannels. Journal of Non-Newtonian Fluid Mechanics. 2009;157(1-2):133-137.
5. Miller SA, Young VY, Martin CR. Electroosmotic flow in template-prepared carbon nanotube membranes. Journal of the American Chemical Society. 2001;123(49):12335-12342.
6. Akbar NS, Nadeem S. Endoscopic effects on peristaltic flow of a nanofluid. Communications in Theoretical Physics. 2011;56(4):761.
7. Noreen S. Mixed convection peristaltic flow of third order Nano fluid with an induced magnetic field. Plos One. 2013;8(11):e78770.
8. Tripathi D, Bég OA. A study on peristaltic flow of nanofluids: Application in drug delivery systems. International Journal of Heat and Mass Transfer. 2014 Mar 1;70:61-70.
9. Reddy MG, Reddy KV. Influence of Joule heating on MHD peristaltic flow of ananofluid with compliant walls. Procedia Engineering. 2015 Jan 1;127:1002-1009.
10. Ebaid A, Aly EH. Additional results for the peristaltic transport of viscous nanofluid in an asymmetric channel with effects of the convective conditions. National Academy Science Letters. 2018;41(1):59-63.
11. Shao Q, Fahs M, Younes A, Makradi A, Mara T. A new benchmark reference solution for double-diffusive convection in a heterogeneous porous medium. Numerical Heat Transfer, Part B: Fundamentals. 2016;70(5):373-392.
12. Huppert HE, Turner JS. Double-diffusive convection. Journal of Fluid Mechanics. 1981 May;106:299-329.
13. Bég OA, Tripathi D. Mathematical simulation of peristaltic pumping with double-diffusive convection in nanofluids: a bio-nano-engineering model. Proceedings of the Institution of Mechanical Engineers, Part N: Journal of Nano engineering and Nanosystems. 2011;225(3):99-114.
14. Kefayati GR. Double-diffusive mixed convection of pseudoplastic fluids in a two sided lid-driven cavity using FDLBM. Journal of the Taiwan Institute of Chemical Engineers. 2014;45(5):2122-2139.
15. Rout BR, Parida SK, Pattanayak HB. Effect of radiation and chemical reaction on natural convective MHD flow through a porous medium with double diffusion. Journal of Engineering Thermophysics. 2014;23(1):53-65.
16. Tripathi D, Mulchandani J, Jhalani S. Electrokinetic transport in unsteady flow through peristaltic microchannel. In AIP Conference Proceedings. AIP Publishing LLC. 2016;1724(1):020043.
17. Tripathi D, Yadav A, Anwar Bég O. Electro-osmotic flow of couple stress fluidsinamicro-channel propagated by peristalsis. The European Physical Journal Plus. 2017;132(4):1-13.
18. Prakash J, Tripathi D. Electroosmotic flow of Williamson ionic nanoliquids in a tapered microfluidic channel in presence of thermal radiation and peristalsis. Journal of Molecular Liquids. 2018 Apr 15;256:352-371.

19. Tripathi D, Yadav A, Bég OA, Kumar R. Study of microvascular non- Newtonian blood flow modulated by electroosmosis. Microvascular Research. 2018 May 1;117:28-36.
20. Tripathi D, Jhorar R, Anwar Bég O, Shaw S. Electroosmosis modulated peristaltic biorheological flow through an asymmetric microchannel: mathematical model. Meccanica. 2018;53(8):2079-2090.
21. Tripathi D, Sharma A, Bég OA. Joule heating and buoyancy effects in electro-osmotic peristaltic transport of aqueous nanofluids through a microchannel with complex wave propagation. Advanced Powder Technology. 2018;29(3):639-653.
22. Waheed S, Noreen S, Hussanan A. Study of heat and mass transfer in electroosmotic flow of third order fluid through peristaltic microchannels. Applied Sciences. 2019;9(10):2164.
23. Noreen S, Tripathi D. Heat transfer analysis on electroosmotic flow via peristaltic pumping in non-Darcy porous medium. Thermal Science and Engineering Progress. 2019 Jun 1;11:254-262.
24. Noreen S, Waheed S, Hussanan A. Peristaltic motion of MHD nanofluid in an asymmetric micro-channel with Joule heating, wall flexibility and different zeta potential. Boundary Value Problems. 2019 Dec;2019(1):1-23.
25. Kefayati GHR. Heat transfer and entropy generation of natural convection on non-Newtonian nanofluids in a porous cavity. Powder technology. 2016 Oct 1;299:127-149.
26. Kefayati GR. Simulation of double diffusive natural convection and entropy generation of power-law fluids in an inclined porous cavity with Soret and Dufour effects (Part II: Entropy generation). International Journal of Heat and Mass Transfer. 2016 Mar 1;94:582-624.
27. Mohan CG, Satheesh A. The numerical simulation of double-diffusive mixed convection flow in a lid-driven porous cavity with magneto hydrodynamic effect. Arabian Journal for Science and Engineering. 2016 May;41(5):1867-1882.
28. Bunonyo KW, Eli IC. Oscillatory Flow of LDL-C and Blood Fluid through a Slanted Channel with Heat within the Sight of Magnetic Field. European Journal of Applied Physics. 2021 Oct 11;3(5):37-44.
29. Bunonyo KW, Amos E. Lipid Concentration Effect on Blood Flow through an Inclined Arterial Channel with Magnetic Field. Mathematical Modelling and Applications. 2020;5(3):129.